TABLE 1. Patient Characteristics

Number	Age	BI	Localization	Size (mm)	Prior Therapy for Lung	Comorbidity
1	78	1200	Carina-rt., main-rt., second carina	35	Rt. B6 segmentectomy, rt. lower lobectomy	HT, cerebrovascular disease
2	56	1050	Lt. B6/basal bronchus spur-B8 + 9/10 spur	15	PDT for lt. second carina and lt. B6, lt. B6 segmentectomy, endobronchial brachytherapy for lt. B6	HT, chronic hepatitis
3	74	1320	Lt. upper bronchus	15	No	HT, COPD, hard of hearing
4	64	800	Rt. middle bronchus	25	PDT for rt. middle bronchus	Gastric ulcer, arrhythmia, COPD
5	80	1200	Rt. main	20	No	COPD
6	74	1000	Lt. upper bronchus	15	No	Renal dysfunction
7	67	800	Rt. basal bronchus	15	Lt. Lower lobectomy	No
8	71	1320	Rt. upper bronchus	25	Carina resection and tracheoplasty, Lt. basal segmentectomy	HT

BI indicates Brinkman Smoking Index; COPD, chronic obstructive pulmonary disease; HT, hypertension; Lt., left; PDT, photodynamic therapy; Rt., right; SCC, squamous cell carcinoma.

distant metastasis (M0) in 8 patients were treated with 3D-CRT with curative intent. Central lung cancer is defined as that originated from airways including and proximal to subsegmental bronchi.[20,21] All lesions were cytologically or histologically proved as squamous cell carcinoma and located from carina up to the segmental bronchus. No tumors could be detected by conventional chest computed tomography (CT). The local spread of the lesions was determined by conventional and autofluorescence bronchoscopy, together with endobronchial ultrasonography. Routine staging of the disease included chest x-rays and CT scans of thorax and abdomen. Brain CT/magnetic resonance imaging and bone scintigraphy/positron emission tomography were not mandatory in the cases of CIS.

Pretreatment characteristics of all 8 patients are shown in Table 1. They were all males and smokers/ex-smokers, whose Brinkman smoking indices were ranged between 800 and 1320. The median age was 71 (range: 56 to 80) years. Eastern Cooperative Oncology Group performance status was 0 in all patients. Most patients were considered to be inoperable, mostly as a result of comorbidities and poor pulmonary function owing to previous surgery, higher age, or chronic obstructive pulmonary disease. Two patients (nos. 1 and 8) experienced stump recurrences at the bronchial resection margins. In 1 patient (no. 7), a new primary lesion appeared away from the stump region. Another one (no. 2) was treated by PDT twice, surgery and endobronchial brachytherapy for the left lower lobe endobronchial cancer, yet developed recurrence. Another one (no. 4) had CIS and received prior PDT for the lesion, but complete regression could not be attained. The remaining 3 patients (nos. 3, 5, and 6) were considered to be inoperable mostly as a result of comorbidities and endobronchial therapy, such as PDT or brachytherapy, was not indicated owing to the extent of the lesions. Patient nos. 3 and 5 had CIS. As conformal radiotherapy (CRT) is considered to be the only available curative treatment, the modality was used after obtaining informed consent.

Treatment

Plain CT images of 0.5-mm thickness were obtained over whole lungs. The images were transferred to radiation planning computer (CADPLAN, Varian Medical Systems, Palo Alto, CA) to make 3D-CRT plans. As the tumor could not be depicted on CT images, clinical target volumes (CTVs) were defined as possible tumor length along the bronchial tree and tumor depth into the bronchial wall on the basis of bronchoscopical findings. Hilar, mediastinal, and supraclavicular nodal regions were not included in CTV. The planning target volume (PTV) was designed by enlarging CTV in all directions by 8 to 10 mm, taking both setup uncertainty and respiratory movement into considerations. Radiation fields were formed with multileaf collimator to achieve conformity with leaf margin of 5 mm and coplanner 5-beams arrangement. Beam energy was 6 or 10 MV x-ray. Figure 1 shows an example of 3D-CRT planning for a central-type lung cancer.

Total 60 Gy, prescribed at the isocenter, was administered by 3-Gy fraction, once a day for 4 weeks. V_{20} of the lungs was defined as the percentage of lung volume that received ≥ 20 Gy radiations in the treatment plan. The biologic effective dose (BED) was calculated using the following formula: $BED = nd\ [1 + d/(\alpha/\beta)]$ where n = number of fractions, d = fraction dose, and α/β is assumed to be 10 for tumor cells or acute responding tissues.

Tumor response was evaluated by bronchoscopy and chest CT. Chest x-ray and CT were examined regularly. Radiation-induced toxicities were graded according to the Radiation Therapy Oncology Group/European Organization for Research and Treatment of Cancer (RTOG/EORTC) Late Radiation Morbidity Scoring Scheme. Pulmonary function tests including percent vital capacity and percent forced expiratory volume in 1 second and arterial blood gas analysis were obtained before and after the treatment to identify the risk factors for lung toxicity by 3D-CRT. Paired t test was used to compare respiratory function and PaO_2 values.

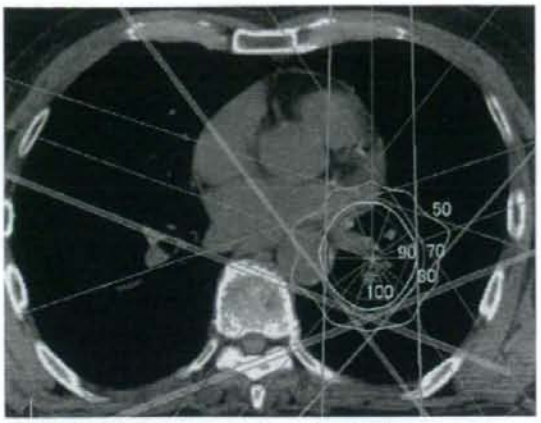

FIGURE 1. The 3-dimensional conformal plan beam arrangement. Circle lines represent the 50% to 100% isodose curves.

RESULTS

The planned treatment was safely performed in all 8 patients with no or minimal acute adverse events. No acute esophageal toxicity was observed. Grade 1 acute radiation pneumonitis (RTOG) was observed in 1 patient. Local response was evaluated by both bronchoscopy and chest CT in 6 patients, but the other 2 patients were considered unsuitable for bronchoscopy and their response was evaluated by sputum cytology and chest CT.

The median follow-up period was 36.8 months (range: 30 to 50 mo). Median survival time was 36.8 months (range: 30 to 50 mo). The 2-year locoregional control rate was 100%. Six patients were alive and 2 died of intercurrent disease without recurrence of centrally located lung cancer. Local failure did not occur in any patient. During follow-up period, secondary lung cancer (adenocarcinoma in both patients) was developed in 2 of 8 patients and they underwent additional 3D-CRT. One of them died of secondary lung cancer due to primary failure at 31 and 10 months after the first and second CRT, respectively. The other patient is alive in the presence of metastasis to the bone and brain, whereas 2 primary sites were maintained to be well controlled in all examinations, including positron emission tomography.

No patient experienced late toxicities at 90 days from the first day of radiation therapy. Table 2 depicts the PTV and the V_{20} values. The median PTV was 45.5 mL (range: 27.6 to 61.8mL) and the median V_{20} value was 10.7% (range: 8.3 to 17.0). We did not encounter interstitial changes in the irradiated lung field with this focal radiation therapy in any of our patients (Figs. 2A, B). Bronchoscopically, the irradiated bronchus was slightly stenotic and scarred (Figs. 3A, B). Respiratory functions and arterial blood gas analysis were unaffected in all patients who underwent the evaluation (Figs. 4A–C). Some patients did experience acute radiation esophagitis, yet it was in grade 2 or less at each occasion.

DISCUSSION

Natural history of CIS and severe dysplasia in the respiratory tract is not clarified completely, and therefore, their treatment strategy is still controversial. Although all of these lesions do not necessarily progress to clinically relevant lung cancers,[22] appreciable proportions of them have high risk of becoming invasive carcinoma. Their risk to progress to a clinical lung cancer was reported to be 33% at 1 year and 54% at 2 years.[23] Therefore, these lesions should be treated in their early stages.

Surgery is the standard treatment for early invasive central airways lung cancer in the patients with good performance status. In Japan, 5-year survival rates of the patients with lung cancer treated surgically are 72% for cIA and 49.9% for cIB and 79.5% for pIA and 60.1% for pIB.[24] On the other hand, Kato et al[1] reported that PDT yielded an initial complete response rate of 84.8% for centrally located early-stage lung cancer. PDT is considered as an effective alternative for surgery for centrally located stage 0 (TisN0M0) and stage I (T1N0M0) early invasive lung cancer, when surgical intervention is difficult or the patients refuse surgery. PDT is especially attractive for elderly patients or those in poor physical condition. Whereas PDT is reported to be effective only for the superficial tumors of < 1 cm in diameter with visible peripheral margin and which is located no more peripherally than subsegmental bronchi, another modality is necessary for the tumors that do not fulfill at least 1 of these conditions.

For many years, the mainstay of treatment for inoperable lung cancer was radiation of nearly 60 Gy of total dose with 2 Gy/fraction over 6 weeks. Conventional external beam radiation of 60 to 70 Gy alone is reported to result in 15% of 5-year overall survival rate, 25% intercurrent death rate, and 50% of treatment failures in local site alone, in the expense of grade 3 to 5 complications of $< 5\%$.[25] These results are not satisfactory for stage I lung cancer. On the basis of dose-response data, Mehta et al[26] estimated that it would take a dose of approximately 85 Gy to achieve 50% long-term control rate using standard 2-Gy daily fractions. It seems that higher doses and shorter treatment times are required to achieve better disease control. However, radiation dose escalation using conventional fractionation and

TABLE 2. Planning Target Volume and V_{20}

Number	PTV (mL)	V_{20} (%)
1	58.24	8.50
2	36.30	9.80
3	36.00	11.78
4	61.80	11.42
5	47.40	9.14
6	36.32	9.35
7	27.60	8.30
8	60.02	16.95

V_{20} was defined as the percentage of lung volume that received ≥ 20 Gy radiations in the treatment plan.
PTV indicates planning target volume.

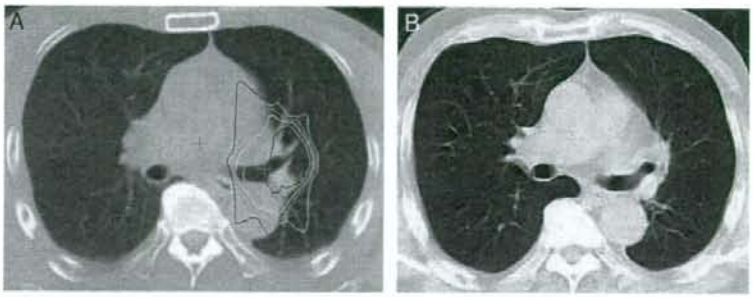

FIGURE 2. A, An example of the dose coverage on an axial CT image in the 74-year-old patient with cancer located at left upper bronchus. B, CT scan at 1-year follow-up shows a complete response without post-treatment interstitial lung changes. CT indicates computed tomography.

techniques would likely cause prohibitive toxicity. 3D-CRT is intended to deliver higher dose of radiation while minimizing damage to surrounding normal tissues. We treated the patients by CRT with 20 fractions of 3 Gy. The biologically effective dose (BED) of this radiation is calculated to be almost equal to 78 Gy in conventional fractionation (assuming α/β of 10). Almost no, at most minimal, interstitial changes were observed in the irradiated lung fields (Figs. 2A, B). This observation was further supported by the fact that respiratory functions were unaffected by the treatment in all patients. These are ascribed to very limited PTV with a median of 45.5 mL. Lagerwaard et al[27] showed that central location of tumors (endobronchial tumor extension) was the only factor that significantly reduced local progression-free survival in 3D-CRT for lung cancer. Our good results can be ascribed to small size of the tumors, which do not require large dose of radiation compared with established invasive cancer. Recently, stereotactic radiotherapy (SRT) is showing favorable results in the treatment of peripherally located stage I lung cancer. Timmerman et al[19] reported a phase 2 trial of SRT with 60 to 66 Gy in 3 fractions during 1 to 2 weeks in 70 patients with medically inoperable early-stage lung cancer. Grade 3 to 5 toxicity occurred in 14 patients (20%). In 2-year follow-up after SRT, 83% of the patients with peripherally located lung cancer experienced no severe complications, whereas 54% of those with centrally located cancer did. The patients with centrally located tumors have 11-fold increased risk of experiencing severe complications compared with those with lung cancer located more peripherally. Their conclusion was that SRT of this regimen should not be used for the patients with tumors located near the central airways because of excessive complications. Similarly, Le et al[28] reported the results of dose-escalation study using single-fraction SRT of 15 to 30 Gy for lung tumors. Majority of the patients who showed grade 2 or greater complications had either centrally located tumors and/or the tumors with treatment volumes greater than 50 mL. The toxicities observed included pneumonitis, pleural effusion, pulmonary embolism, and tracheoesophageal fistula. These results indicate that high-dose radiation by limited fractions is dangerous for perihilar structure of the lung. As small lung cancer,

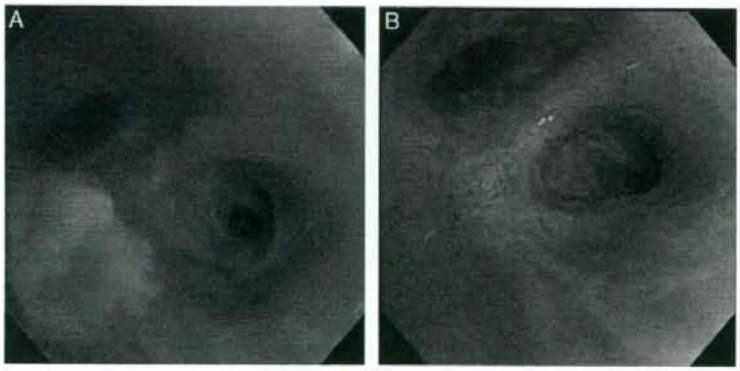

FIGURE 3. A case of 74-year-old patient with central type lung cancer. A, Squamous cell carcinoma located at left upper bronchus. B, After 6 months of 3D-CRT, the irradiated bronchus was slightly stenotic and scarred. 3D-CRT indicates 3-dimensional conformal radiotherapy.

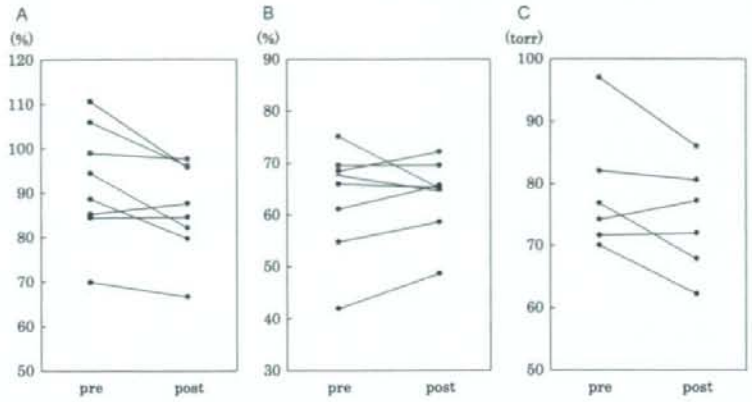

FIGURE 4. Respiratory function values of preradiotherapy and postradiotherapy. A, %VC: percent vital capacity. B, FEV1.0%: percent forced expiratory volume in 1 second. C, PaO_2: arterial blood gas analysis.

such as CIS and early invasive cancer, is curative by radiation with sufficient dose, determination of total dose and fractionation is critical to treat small lung cancer located in the central airways. Although the number of the patients entered into this study is small, our method may afford a good clue.

CONCLUSIONS

As small lung cancer, such as CIS and early invasive cancer, is curative by radiation with sufficient dose, determination of total dose and fractionation is critical to treat small lung cancer located in the central airway. 3D-CRT given by 20 fractions of 3 Gy is a safe and effective treatment for inoperable CIS or early invasive central airways lung cancer.

REFERENCES

1. Kato H, Usuda J, Furukawa K, et al. Basic and clinical research on photodynamic therapy at Tokyo Medical University Hospital. *Lasers Surg Med*. 2006;38:371–375.
2. Hennequin C, Bleichner O, Tredaniel J, et al. Long-term results of endobronchial brachytherapy: a curative treatment? *Int J Radiat Oncol Biol Phys*. 2007;67:425–430 [Epub November 2, 2006].
3. Zhang HX, Yin WB, Zhang LJ, et al. Curative radiotherapy of early operable non-small cell lung cancer. *Radiother Oncol*. 1989;14: 89–94.
4. Talton BM, Constable WC, Kersh CR. Curative radiotherapy in non-small cell carcinoma of the lung. *Int J Radiat Oncol Biol Phys*. 1990;19:15–21.
5. Dosoretz DE, Katin MJ, Blitzer PH, et al. Radiation therapy in the management of medically inoperable carcinoma of the lung: results and implications for future treatment strategies. *Int J Radiat Oncol Biol Phys*. 1992;24:3–9.
6. Dosoretz DE, Galmarini D, Rubenstein JH, et al. Local control in medically inoperable lung cancer: an analysis of its importance in outcome and factors determining the probability of tumor eradication. *Int J Radiat Oncol Biol Phys*. 1993;27:507–516.
7. Kaskowitz L, Graham MV, Emami B, et al. Radiation therapy alone for stage I non-small cell lung cancer. *Int J Radiat Oncol Biol Phys*. 1993;27:517–523.
8. Slotman BJ, Nio KH, Karim AB. Curative radiotherapy for technically operable stage I nonsmall cell lung cancer. *Int J Radiat Oncol Biol Phys*. 1994;29:33–37.
9. Graham PH, Gebski VJ, Langlands AO. Radical radiotherapy for early nonsmall cell lung cancer. *Int J Radiat Oncol Biol Phys*. 1995; 31:261–266.
10. Gauden S, Ramsay J, Tricony L. The curative treatment by radiotherapy alone of stage I non-small cell carcinoma of the lung. *Chest*. 1995;108:1278–1282.
11. Furuta M, Hayakawa K, Katano S, et al. Radiation therapy for stage I-II non-small cell lung cancer in patients aged 75 years and older. *Jpn J Clin Oncol*. 1996;26:95–98.
12. Gauden SJ, Tripcony L. The curative treatment by radiation therapy alone of stage I non-small cell lung cancer in a geriatric population. *Lung Cancer*. 2001;32:71–79.
13. Sibley GS, Jamieson TA, Marks LB, et al. Radiotherapy alone for medically inoperable stage I non-small-cell lung cancer: the Duke experience. *Int J Radiat Oncol Biol Phys*. 1998;40:149–154.
14. Hayakawa K, Mitsuhashi N, Saito Y, et al. Limited field irradiation for medically inoperable patients with peripheral stage I non-small cell lung cancer. *Lung Cancer*. 1999;26:137–142.
15. Morita K, Fuwa N, Suzuki Y, et al. Radical radiotherapy for medically inoperable non-small cell lung cancer in clinical stage I: a retrospective analysis of 149 patients. *Radiother Oncol*. 1997;42: 31–36.
16. Cheung PC, Mackillop WJ, Dixon P, et al. Involved-field radiotherapy alone for early-stage non-small-cell lung cancer. *Int J Radiat Oncol Biol Phys*. 2000;48:703–710.
17. Jeremic B, Classen J, Bamberg M. Radiotherapy alone in technically operable, medically inoperable, early-stage (I/II) non-small-cell lung cancer. *Int J Radiat Oncol Biol Phys*. 2002;54:119–130.
18. Rosenzweig KE, Dladla N, Schindelheim R, et al. Three-dimensional conformal radiation therapy (3D-CRT) for early-stage non-small-cell lung cancer. *Clin Lung Cancer*. 2001;3:141–144.
19. Timmerman R, McGarry R, Yiannoutsos C, et al. Excessive toxicity when treating central tumors in a phase II study of stereotactic body radiation therapy for medically inoperable early-stage lung cancer. *J Clin Oncol*. 2006;24:4833–4839.
20. The Japan Lung Cancer Society. *In General Rule for Clinical and Pathological Record of Lung Cancer (The 6th edn)*. Japan: Kanehara & Co Ltd; 2003:83–92.

21. Kennedy TC, McWilliams A, Edell E, et al. Bronchial Intraepithelial Neoplasia/Early Central Airways Lung Cancer: ACCP Evidence-Based Clinical Practice Guidelines (2nd edn). *Chest*. 2007;132: 221–233.
22. Auerbach O, Stout AP, Hammond EC, et al. Changes in bronchial epithelium in relation to cigarette smoking and in relation to lung cancer. *N Engl J Med*. 1961;265:253–267.
23. Jeremy George P, Banerjee AK, Read CA, et al. Surveillance for the detection of early lung cancer in patients with bronchial dysplasia. *Thorax*. 2007;62:43–50 [Epub July 6, 2006].
24. Goya T, Asamura H, Yoshimura H, et al. Prognosis of 6644 resected non-small cell lung cancers in Japan: a Japanese lung cancer registry study. *Lung Cancer*. 2005;50:227–234 [Epub August 2, 2005].
25. Sibley GS. Radiotherapy for patients with medically inoperable Stage I nonsmall cell lung carcinoma: smaller volumes and higher doses—a review. *Cancer*. 1998;82:433–438.
26. Mehta M, Scrimger R, Mackie R, et al. A new approach to dose escalation in non-small-cell lung cancer. *Int J Radiat Oncol Biol Phys*. 2001;49:23–33.
27. Lagerwaard FJ, Senan S, van Meerbeeck JP, et al. Has 3-D conformal radiotherapy (3D CRT) improved the local tumour control for stage I non-small cell lung cancer? *Radiother Oncol*. 2002;63:151–157.
28. Le QT, Loo BW, Cotrutz C, et al. Results of a phase I dose-escalation study using single-fraction stereotactic radiotherapy for lung tumors. *J Thorac Oncol*. 2006;1:802–809.

Oncogene (2009) 28, 518–533

www.nature.com/onc

ORIGINAL ARTICLE

Disruption of the EGFR E884–R958 ion pair conserved in the human kinome differentially alters signaling and inhibitor sensitivity

Z Tang[1], S Jiang[1], R Du[1], ET Petri[2], A El-Telbany[1], PSO Chan[3], T Kijima[4], S Dietrich[1], K Matsui[5], M Kobayashi[5], S Sasada[5], N Okamoto[5], H Suzuki[5], K Kawahara[6], T Iwasaki[7], K Nakagawa[7], I Kawase[4], JG Christensen[8], T Hirashima[5], B Halmos[1], R Salgia[9], TJ Boggon[2], JA Kern[10] and PC Ma[1]

[1]*Division of Hematology/Oncology, Case Western Reserve University School of Medicine, University Hospitals Case Medical Center and Ireland Cancer Center, Case Comprehensive Cancer Center, Cleveland, OH, USA;* [2]*Department of Pharmacology, Yale University School of Medicine, New Haven, CT, USA;* [3]*Elpidex Bioscience Inc., Los Angeles, CA, USA;* [4]*Department of Respiratory Medicine, Allergy and Rheumatic Diseases, Osaka University Graduate School of Medicine, Osaka, Japan;* [5]*Department of Thoracic Malignancy, Osaka Prefectural Medical Center for Respiratory and Allergic Disease, Osaka, Japan;* [6]*Department of Pathology, Osaka Prefectural Medical Center for Respiratory and Allergic Disease, Osaka, Japan;* [7]*Department of Thoracic Surgery, Osaka Prefectural Medical Center for Respiratory and Allergic Disease, Osaka, Japan;* [8]*Pfizer Inc., Global Research and Development, San Diego, CA, USA;* [9]*Section of Hematology/Oncology, University of Chicago Pritzker School of Medicine, University of Chicago Cancer Research Center, Chicago, IL, USA and* [10]*Division of Pulmonary, Critical Care and Sleep Medicine, Case Western Reserve University School of Medicine, University Hospitals Case Medical Center and Ireland Cancer Center, Case Comprehensive Cancer Center, Cleveland, OH, USA*

Targeted therapy against epidermal growth factor receptor (EGFR) represents a major therapeutic advance in lung cancer treatment. Somatic mutations of the *EGFR* gene, most commonly L858R (exon 21) and short in-frame exon 19 deletions, have been found to confer enhanced sensitivity toward the inhibitors gefitinib and erlotinib. We have recently identified an EGFR mutation E884K, in combination with L858R, in a patient with advanced lung cancer who progressed on erlotinib maintenance therapy, and subsequently had leptomeningeal metastases that responded to gefitinib. The somatic E884K substitution appears to be relatively infrequent and resulted in a mutant lysine residue that disrupts an ion pair with residue R958 in the EGFR kinase domain C-lobe, an interaction that is highly conserved within the human kinome as demonstrated by our sequence analysis and structure analysis. Our studies here, using COS-7 transfection model system, show that E884K works in concert with L858R in-*cis*, in a dominant manner, to change downstream signaling, differentially induce Mitogen-activated protein kinase (extracellular signaling-regulated kinase 1/2) signaling and associated cell proliferation and differentially alter sensitivity of EGFR phosphorylation inhibition by ERBB family inhibitors in an inhibitor-specific manner. Mutations of the conserved ion pair E884–R958 may result in conformational changes that alter kinase substrate recognition. The analogous E1271K-MET mutation conferred differential sensitivity toward preclinical MET inhibitors SU11274 (unchanged) and PHA665752 (more sensitive). Systematic bioinformatics analysis of the mutation catalog in the human kinome revealed the presence of cancer-associated mutations involving the conserved E884 homologous residue, and adjacent residues at the ion pair, in known proto-oncogenes (*KIT*, *RET*, *MET* and *FAK*) and tumor-suppressor gene (*LKB1*). Targeted therapy using small-molecule inhibitors should take into account potential cooperative effects of multiple kinase mutations, and their specific effects on downstream signaling and inhibitor sensitivity. Improved efficacy of targeted kinase inhibitors may be achieved by targeting the dominant activating mutations present.

Oncogene (2009) **28,** 518–533; doi:10.1038/onc.2008.411; published online 17 November 2008

Keywords: *EGFR*; *MET*; mutation; tyrosine kinase inhibitor; structure; kinome

Introduction

Targeted therapy using epidermal growth factor receptor (EGFR) kinase inhibitors represents a major therapeutic advance in lung cancer treatment. Somatic mutations of the *EGFR* gene, most commonly L858R (exon 21) and short in-frame deletions in exon 19, have recently been identified as catalytic domain mutation hotspots (Shigematsu and Gazdar, 2006). These mutations confer enhanced sensitivity toward the anilinoquinazoline kinase inhibitors gefitinib and erlotinib (Lynch *et al.*, 2004;

Correspondence: Dr PC Ma, Division of Hematology/Oncology, Case Western Reserve University School of Medicine, University Hospitals Case Medical Center and Ireland Cancer Center, Case Comprehensive Cancer Center, 10900 Euclid Avenue, WRB 2-123, Cleveland, OH 44106, USA.
E-mail: patrick.ma@case.edu
Received 10 March 2008; revised 17 September 2008; accepted 1 October 2008; published online 17 November 2008

Paez *et al*., 2004). A mutation conferring resistance to these two kinase inhibitors, T790M (exon 20), has also been found in the EGFR kinase domain and can account for about half of the cases of acquired resistance (Kobayashi *et al*., 2005). There are a number of other kinase domain mutations of EGFR that occur at lower frequencies, most often in combination with L858R (Tam *et al*., 2006). However, how these mutations might interact when present together in-*cis* is unknown.

We recently identified a novel EGFR kinase domain somatic mutation, E884K (Glu884Lys, exon 22) in a patient with stage IV non-small-cell lung cancer, in combination with the L858R mutation (L858R + E884K) (Choong *et al*., 2006). The patient initially received carboplatin/paclitaxel and erlotinib and then developed brain metastasis on maintenance erlotinib. In spite of further treatment with whole brain radiation, temozolomide and irinotecan, the patient's disease progressed to symptomatic leptomeningeal carcinomatosis, which responded to gefitinib, a year after being off an EGFR kinase inhibitor. The L858R + E884K double mutation was found both in her pretreatment diagnostic thoracic lymph node biopsy specimen as well as in the tumor cells (extracted by laser microdissection) within the cerebrospinal fluid during the course of leptomeningeal metastases (Choong *et al*., 2006). The E884K mutation represents the first mutation reported to show an apparent differential response to the two EGFR kinase inhibitors erlotinib and gefitinib, whereas L858R was known to be sensitizing to both. These findings led to our hypothesis that EGFR kinase mutations can work together to differentially alter inhibitor sensitivity and downstream signaling. Further biochemical analysis in our current study indicates that the double mutant EGFR (L858R + E884K) responds differently to gefitinib and erlotinib. We now show that E884K works in concert with L858R, and in a dominant manner, to mediate differential sensitivity to kinase inhibitors through altered phosphorylation of AKT and signal transducer and activator of transcription 3 (STAT3) and were correlated with differential cellular cytotoxicity and induction of the apoptotic marker cleaved-PARP(Asp214) by EGFR inhibitors. Using a combination of bioinformatics and structural analyses, we further characterized the role of the E884 residue in EGFR kinase function. Our results further demonstrate that the ion pair formed by residues E884 and R958 in the EGFR kinase domain is a highly conserved feature of protein kinases in the human kinome, including many 'druggable' targets such as MET. Disruption of the conserved ion pair in EGFR modulates downstream signal transduction and differentially alters kinase inhibitor sensitivity in an inhibitor-specific manner.

Results

E884K works in concert with L858R mutation to confer differential inhibitor sensitivity through inhibition of AKT and STAT3 downstream signaling

We hypothesize that EGFR kinase mutations can work together to differentially alter inhibitor sensitivity. To test this hypothesis, *EGFR* expression constructs engineered with L858R (LR) or dual mutations of L858R + E884K (LR + EK) were stably transfected into COS-7 cells. Cells were treated with increasing concentrations of either erlotinib or gefitinib in the presence of EGF stimulation (Figure 1a). Compared with L858R alone, the L858R + E884K dual mutant was less sensitive to erlotinib in the inhibition of tyrosine phosphorylation of EGFR. Conversely, E884K worked in concert with L858R in-*cis* to further enhance the sensitivity of the mutant receptor to gefitinib inhibition (Figures 1a and b). These findings correlated with the clinical course of the patient's response profile (Choong *et al*., 2006) and highlight the potential for EGFR kinase mutations to exert concerted effects in-*cis* to impact targeted inhibition.

To gain insight into the mechanism of E884K modulation of EGFR tyrosine kinase inhibitor (TKI) sensitivity, we further studied its effect on downstream AKT and STAT3 signaling pathways with TKI inhibition. The effect on the downstream signal mediators p-AKT (S473) and p-STAT3 (Y705) correlated well with the inhibition of EGFR phosphorylation (Figure 1a); E884K in-*cis* with L858R decreased erlotinib inhibition of AKT and STAT3 phosphorylation but increased inhibition by gefitinib. The differential inhibition exerted by E884K on EGFR, AKT and STAT3 signaling also corresponded to the inhibitor-induced expression pattern of the apoptotic marker, cleaved-PARP(Asp214) (Figure 1c). Similarly, there was an opposite effect of the E884K mutation over L858R in-*cis* in inducing cellular cytotoxicity by erlotinib and gefitinib (Figure 1d). Hence, E884K in-*cis* with L858R differentially altered inhibitor sensitivity when compared with L858R alone, through differential inhibition of the prosurvival AKT and STAT3 signaling pathways associated with altered induction of cleaved-PARP(Asp214).

E884K-EGFR modulates inhibitor sensitivity effects in an inhibitor-specific manner

To further examine the hypothesis that EGFR mutations exert effects in combination that are unique to a specific kinase inhibitor, we further tested the mutant EGFR expressing L858R alone or L858R + E884K in-*cis*, against several other ERBB family TKIs, including both reversible inhibitors (4557W, Lapatinib, GW583340, Tyrphostin-AG1478) and irreversible inhibitor (CL-387,785) (Figure 2 and Supplementary Figure 2). We focused on the effects of these inhibitors on the sensitivity of inhibition of the EGFR kinase phosphorylation in the mutant EGFR. As the tyrosine phosphorylation of the EGFR has been shown to correlate well with its catalytic enzymatic activity, we used the tyrosine phosphorylation of the pY1068 (GRB1-binding site) epitope of EGFR as the surrogate measurement of the extent of inhibition by the TKIs. For 4557W (reversible dual TKI of EGFR/ERBB2), the E884K mutation modulated the L858R mutation in-*cis*, again in a dominant manner, rendering the double-mutant receptor more sensitive to the dual inhibitor

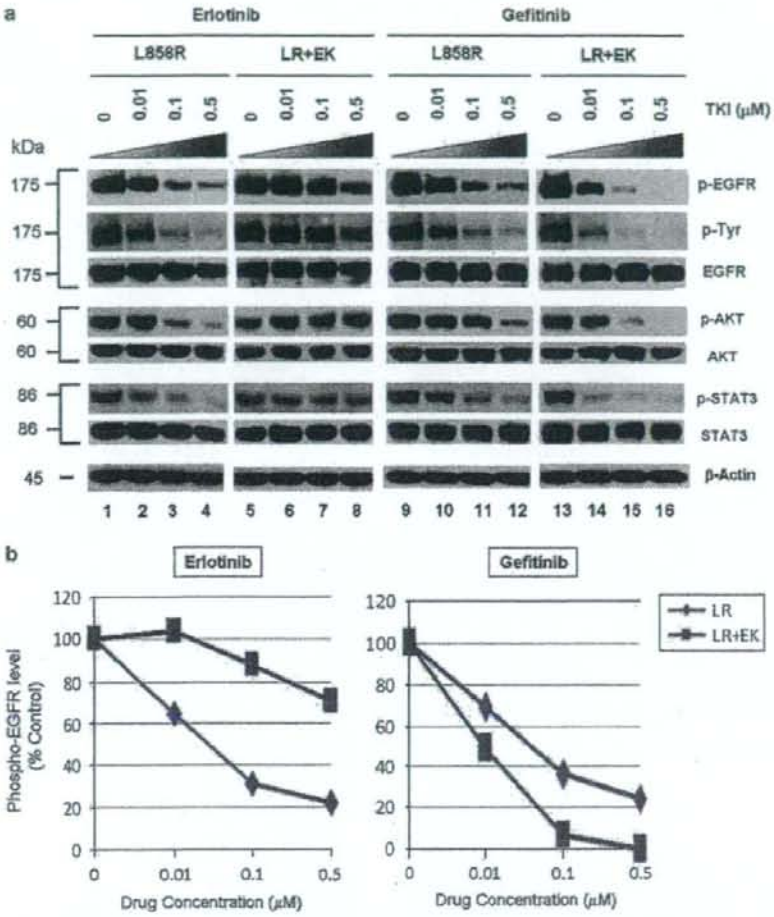

Figure 1 E884K mutation of epidermal growth factor receptor (EGFR) worked in concert with L858R to differentially alter sensitivity to EGFR kinase inhibitors erlotinib and gefitinib. (**a**) Stable COS-7 transfects expressing the L858R and double-mutant L858R + E884K variants of *EGFR* were used in the experiment. The endogenous wild-type EGFR expression of parental COS-7 cells is negligible (data not shown). Cells were cultured in 0.5% bovine serum albumin-containing serum-free media for 16 h and then incubated with increasing concentrations of either erlotinib or gefitinib in the presence of EGF (100 ng/ml). Whole-cell lysates were extracted for SDS polyacrylamide gel electrophoresis and immunoblotting using antibodies against: p-EGFR (Y1068), phosphotyrosine (p-Tyr), EGFR, p-AKT (S473), AKT, p-STAT3 (Y705), STAT3 and β-actin. The experiment was performed in duplicate with reproducible results. The E884K mutation negatively modulated the effect of L858R to erlotinib inhibition in a dominant manner but enhanced sensitivity of the mutant receptor to gefitinib inhibition. (**b**) Densitometric quantitation of the p-EGFR (Y1068) levels showing differential alteration of sensitivity to erlotinib (more resistant) and gefitinib (more sensitive) by the E884K mutation when in-*cis* with L858R. The densitometric scanning of the p-EGFR immunoblot bands was performed digitally using the NIH ImageJ software program and was normalized to the total EGFR expression levels. (**c**) Relative expression of the apoptotic marker cleaved-PARP(Asp214) in L858R and L858R + E884K *EGFR* variants treated with increasing concentrations of erlotinib (left) and gefitinib (right). The immunoblot from whole cell lysates as in (**a**), using anti-cleaved-PARP(Asp214) (c-PARP) antibody is shown here (above) together with the densitometric quantitation (below) adjusted to β-actin loading control using the NIH ImageJ software program. (**d**) COS-7 cells with stable transduced expression of L858R or L858R + E884K mutant *EGFR* were tested in cellular cytotoxicity assay *in vitro* under drug treatment with either erlotinib or gefitinib at indicated concentrations. Results are shown in percentage change of cell viability of L858R + E884K EGFR-COS-7 compared with the control L858R EGFR-COS-7 cells at each concentration of TKI tested. E884K mutation, when in-*cis* with L858R, significantly decreased the sensitivity of cell viability inhibition by erlotinib compared with L858R alone; however, it significantly increased the sensitivity of cell viability inhibition by gefitinib compared with L858R alone. In the case of erlotinib, E884K was desensitizing to L858R, leading to lower cytotoxicity (56.3 ± 2.68% increased viable cells after inhibition at 5 μM, $P = 0.0004$) compared with L858R alone. Conversely, in gefitinib inhibition, E884K further sensitized L858R in-*cis*, leading to significantly higher cytotoxicity (63.5 ± 6.86% decreased viable cells after inhibition at 5 μM, $P = 0.0013$) compared with L858R alone. Error bar, s.d. ($N = 3$). *$P < 0.05$, compared with L858R alone. Representative photomicrographs of cells after 48 h of indicated inhibitor treatment (5 μM) *in vitro* were included to illustrate the presence of differential cytotoxicity as seen with the nonviable detached cells or cell fragments (× 10). Examples of increased floating nonviable cells are highlighted with arrows.

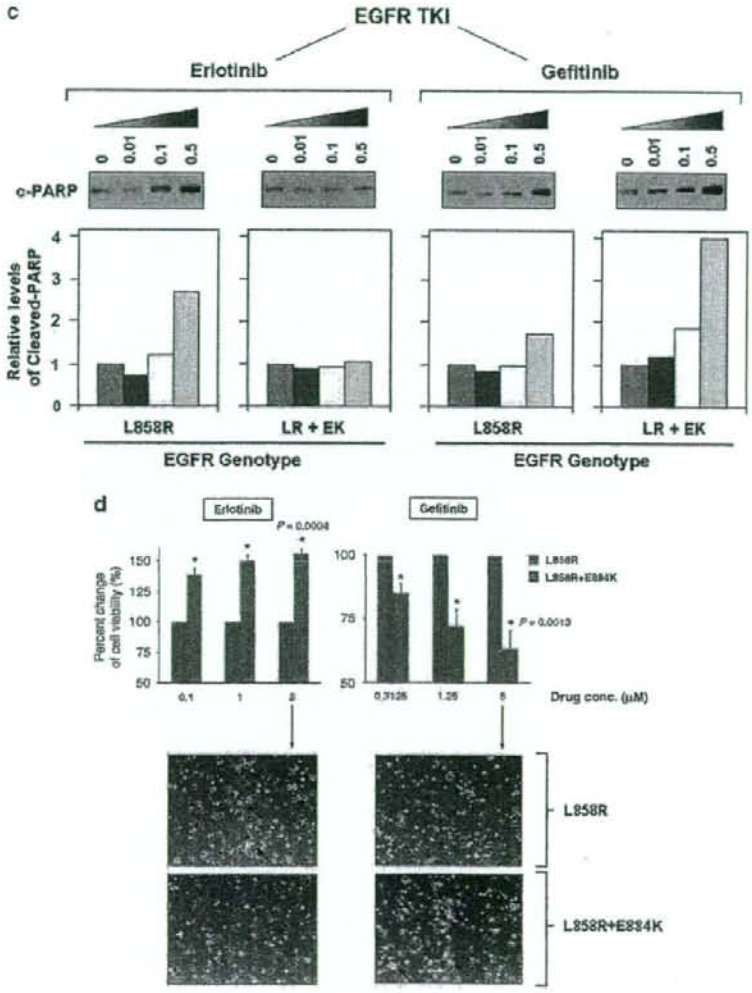

Figure 1 Continued.

(Figure 2). Hence, E884K mutation can work in concert with L858R to modulate mutant receptor sensitivity to different targeted inhibitors. Similarly, E884K further enhanced the sensitivity of L858R to the inhibition by the irreversible EGFR/ERBB2 inhibitor, CL-387,785. On the other hand, the sensitivity of EGFR phosphorylation between the L858R and L858R + E884K EGFR receptors in Tyrphostin-AG1478 (reversible EGFR-TKI), GW583340 (reversible dual EGFR/ERBB2-TKI) and lapatinib (reversible dual EGFR/ERBB2-TKI) did not significantly differ. Hence, the E884K mutation, when in-*cis* with L858R, modulates the sensitivity of the mutant receptor toward ERBB family kinase inhibitors in an inhibitor-specific manner.

E884K is activating, and can work cooperatively with L858R to differentially modulate downstream signal transduction

To address the question whether there are other downstream phosphoproteins that can be differentially activated by the E884K mutation compared with the activating L858R mutation, the global phosphotyrosine profiles of the cellular proteins induced by the mutant EGFR were examined. The E884K alone and L858R + E884K double-mutant EGFR remained sensitive to EGF, and the E884K mutation cooperates with L858R when in-*cis* to further enhance the mutational effects on downstream phosphoprotein activation (data not shown). To date, essentially all mutational combinations involving L858R studied thus far were found to

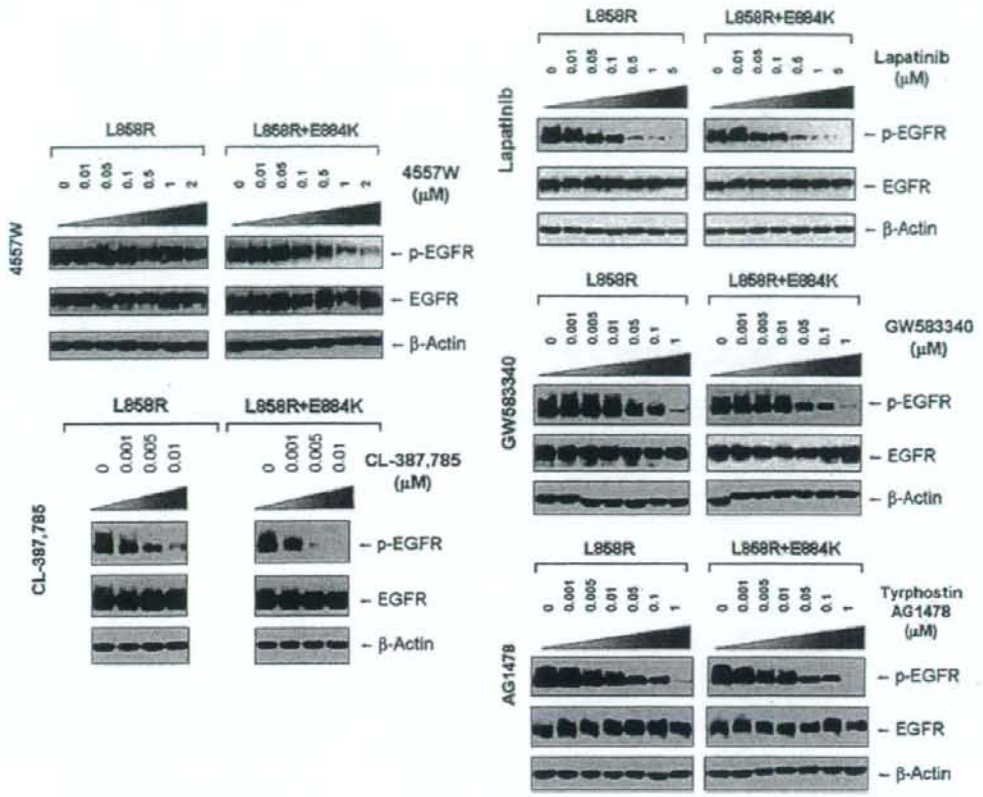

Figure 2 Effects of L858R/E884K-EGFR on other epidermal growth factor receptor (EGFR) kinase inhibitors. The EGFR mutation E884K modulated L858R mutation in-*cis* with inhibitor-specific effects on the sensitivities to EGFR phosphorylation inhibition by the inhibitors (4557W, GW583340, Tyrphostin-AG1478, lapatinib and CL-387,785). Stable COS-7 transfectant cells expressing equivalent levels of the following *EGFR* variants were used: L858R (LR) and L858R + E994K (LR + EK). Cells were cultured in 0.5% bovine serum albumin-containing serum-free media for 16 h, and then treated with or without increasing concentrations of the EGFR TKIs as indicated, in the presence of EGF stimulation (100 ng/ml). Whole cell lysates were extracted for SDS polyacrylamide gel electrophoresis and immunoblotting using the following antibodies: p-EGFR (Y1068), EGFR and β-actin. E884K mutation worked in concert with L858R in-*cis* to enhance the sensitivity of the mutant receptor to inhibition by the kinase inhibitor 4557W, and CL-387,785. On the other hand, it has little effects on the inhibition by lapatinib, GW583340 and Tyrphostin-AG1478.

exist in-*cis*, suggesting potential *cis* mutation-to-mutation cooperation in EGFR signaling and possibly tumorigenesis (Tam *et al*., 2006). To determine the effect of E884K on mutant EGFR signaling, we next studied the EGFR activation of the downstream PI3K-AKT-MAPK (ERK1/2)-STAT pathway. E884K mutant (alone or in-*cis* with L858R) receptor exhibited constitutive activation of the tyrosine phosphorylated EGFR comparable with L858R (Figure 3a). E884K and L858R + E884K mutants remained sensitive to EGF and were activated by the ligand to a level comparable with L858R (Figure 3a). L858R was associated with downstream activation of p-AKT signaling, which was inducible by EGF stimulation. When in-*cis* with L858R, E884K mutation (L858R + E884K) downregulated constitutive AKT phosphorylation. E884K, alone or in-*cis* with L858R, can also mediate constitutive induction of p-STAT3 (pY705) (important for STAT3 dimerization and transcriptional activation of target genes) (Figure 3a). Interestingly, the double mutation L858R + E884K conferred a distinctly more sensitive response to EGF stimulation selectively in the mitogen-activated protein kinase (extracellular signaling-regulated kinase 1/2) (MAPK-ERK1/2) cell proliferation pathway compared with either wild type, E884K alone or L858R alone. Consistent with this differential signaling effect, the L858R + E884K-COS-7 cells had a significantly higher cell proliferation rate than that of the L858R-COS-7 cells in the MTS cell proliferation assay for 5 days (Figure 3b). At days 3 and 5, the cell proliferation rate as determined by % viable cell increase during the assay period was 1.46-fold (day 3) and 1.40-fold ($P = 0.0013$) higher (day 5) in L858R + E884K than L858R alone. L858R + E884K

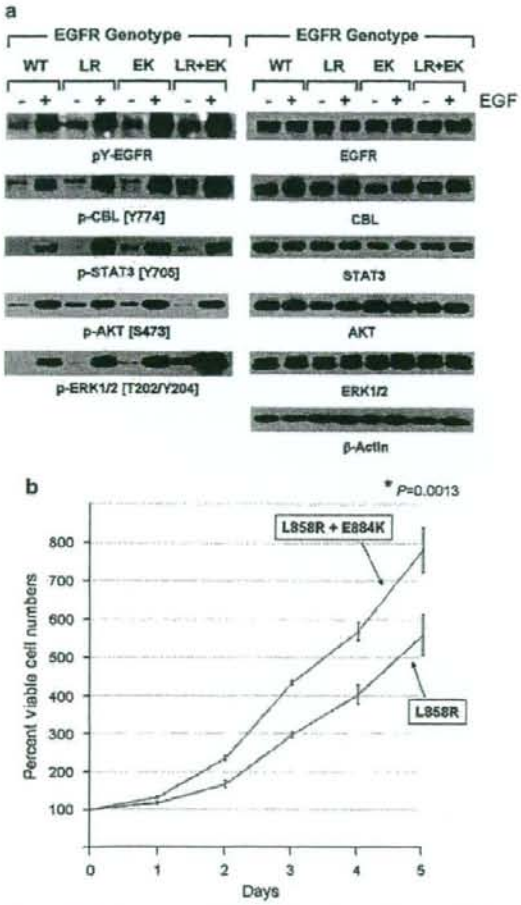

Figure 3 Effects of mutational disruption of the Glu(E)884 Arg(R)958 ion pair in epidermal growth factor receptor (EGFR) signaling. (**a**) Stable COS-7 transfectant cells expressing the various *EGFR* variants were cultured in 0.5% bovine serum albumin-containing serum-free media, followed by EGF stimulation (100 ng/ml, 10 min). Whole cell lysates were prepared for SDS polyacrylamide gel electrophoresis and immunoblotted using the antibodies against: phosphotyrosine (pY-EGFR), EGFR, p-CBL (Y774), CBL, p-STAT3 (Y705), STAT3, p-AKT (S473), AKT, p-ERK1/2 (T202/Y204), ERK1/2 and β-actin. E884K, either alone or in-*cis* with L858R, modulated differential activation of downstream mutant EGFR signaling. (**b**) The EGFR double mutations L858R + E884K conferred a significantly higher cell proliferation rate than L858R alone in the COS-7 cells stably expressing the transduced mutant *EGFR*. Cellular viability assay was performed with the cells growing in regular growth media (10% fetal bovine serum) up to 5 days as described in Materials and methods. The MTS viability assay was performed in triplicate. Error bar, s.d. $^*P = 0.0013$.

also conferred a higher induction of p-CBL as well. Hence, the double mutation L858R + E884K modulated basal and stimulated downstream EGFR signaling differentially with differential effects on the AKT (downregulated), CBL and MAPK-ERK1/2 phosphorylation (upregulated). Moreover, E884K had a dominant effect over L858R, when in-*cis*, in these signaling modulatory effects.

Disruption of a conserved ion pair, Glu(E)884-Arg(R)958, in EGFR differentially alters kinase inhibitor sensitivity

Next, bioinformatics analysis of the E884 residue was performed by multiple kinase domain amino-acid sequence alignments of the human kinome, using the AliBee multiple sequence alignment program (GeneBee, Moscow, Russia) (Supplementary Figure 1). Amino-acid alignments of the kinase domains of phylogenetically diverse groups of kinases such as among the ERBB family, the vascular endothelial growth factor receptor family and the TRK family show that the E884 residue is highly conserved (Figure 4a). In addition, a second residue was also found to be highly conserved (R958) (Figure 4a). Further multiple sequence alignments of 321 human kinase domains show high conservation of both E884 and R958 residues of the EGFR kinase domain (Supplementary Figure 1). The glutamic acid residue (E884) is conserved in >77% and the arginine residue (R958) is conserved in >55% of human kinases in the kinome.

Finally, we mapped the locations of the L858R and E884K mutations onto the three-dimensional structure of the EGFR kinase domain complexed with erlotinib and with lapatinib (PDB accession codes 1M17 (Stamos *et al*., 2002) and 1XKK (Wood *et al*., 2004)) (Figure 4b). We also generated a superposition of the EGFR kinase domain with multiple diverse kinase catalytic domains (Figure 4c). These analyses show the structural conservation of the buried Glu(E)-Arg(R) ion pair and that the exon 22 residue, E884, is physically distant from L858 in exon 21. Furthermore, unlike L858, E884 is not proximal to the adenosine triphosphate-binding cleft of the kinase domain, making it difficult to predict its effects on kinase inhibitor interactions. Mutation of the acidic glutamate residue at codon 884 to a basic lysine will disrupt the highly conserved ion pair through charge–charge repulsion with the basic residue R958 (Figures 4b and c).

To further test the hypothesis of the disruption of the conserved E884–R958 salt bridge as a mechanism underlying the differential response of the mutant EGFR to kinase inhibitors, we tested the double mutant L858R + R958D against erlotinib and gefitinib (Figure 5). Substitution of the wild-type Arg(R)958 with Asp(D)958 was created using site-directed mutagenesis. We hypothesized that the R958D substitution would disrupt the ion pair with E884 through electrostatic repulsion, in a way similar to the effect of the E884K substitution. COS-7 cells transfected to express the indicated mutant EGFR receptors were inhibited using either erlotinib or gefitinib *in vitro* with increasing concentrations. Similar to E884K, R958D modulated the sensitizing effect of L858R differentially to reversible EGFR inhibitors when in-*cis* (with L858R). R958D mutation, when in-*cis* with L858R, decreased the

sensitivity of the mutant receptor to erlotinib inhibition, while increasing the sensitivity to gefitinib in a dominant manner (Figures 5a and b).

Mutational disruption of the conserved kinase ion pair in MET kinase by E1271K-MET also differentially alters the sensitivity of phosphorylation inhibition by MET inhibitors

MET has been shown to play a key role in the development of many human malignancies. A number of mutations have been identified in *MET* from various cancers. Recently, it has been shown that MET represents a key oncogenic signaling in lung cancer alongside with EGFR signaling (Rikova *et al.*, 2007; Guo *et al.*, 2008; Tang *et al.*, 2008). Moreover, MET can cross-activate with EGFR when they are co-expressed, which happens rather frequently (Rikova *et al.*, 2007; Tang *et al.*, 2008). MET has also been shown to be an attractive therapeutic molecular target (Ma *et al.*, 2003b; Shinomiya *et al.*, 2004; Mazzone and Comoglio, 2006; Peruzzi and Bottaro, 2006; Smolen *et al.*, 2006). Here, we test the hypothesis that E1271K mutation of *MET*, analogous to E884K-*EGFR*, can also differentially alter inhibitory sensitivity toward selective MET inhibitors (Figure 6). The Glu(E)1271-Arg(R)1345 constitutes the conversed ion-pair in MET kinase (Figures 4 and 6). The location of the E1271–R1234 ion pair in MET kinase is illustrated in the recently reported crystallographic structure of the MET kinase domain complexed with SU11274 (Bellon *et al.*,

Figure 4 The ion pair Glu(E)884-Arg(R)958 in the epidermal growth factor receptor (EGFR) kinase domain is a highly conserved feature in the human kinome. (**a**) A selected list of 32 diverse human protein kinases with known importance as validated or potential cancer therapeutic targets was included here with bioinformatics alignment analysis of the kinase domain amino-acid sequences. Glu884 (E884) and Arg958 (R958) of EGFR are both highly conserved residues among these kinases. (Left) Amino-acid alignment of the kinase domains of 32 diverse members of human protein kinases showing E884-EGFR is highly conserved: EGFR, ERBB2, ERBB3, ERBB4, RON, MET, TYRO3, MER, AXL, RYK, RET, FGFR1, FGFR2, FGFR3, FLT3, KIT, PDGFR-A, PDGFR-B, vascular endothelial growth factor receptor-1, vascular endothelial growth factor receptor-2, vascular endothelial growth factor receptor-3, SRC, EPHA2, EPHB2, FAK, ZAP70, TRK-A, TRK-B, TRK-C, IGFR1, ALK and c-ABL. (Right) R958-EGFR is also highly conserved among diverse members of kinases. For the complete alignment analysis of kinase domains of the human kinome, see Supplementary Figure 1. (**b**) EGFR kinase domain crystal structures (PDB accession codes 1M17 (Stamos *et al.*, 2002) and 1XKK (Wood *et al.*, 2004)) when in complex with erlotinib (blue) and lapatinib (green) are shown. The locations of L858 (exon 21) and E884 (exon 22) are highlighted. E884 (acidic) and R958 (basic) residues form an ion pair in wild-type EGFR that would be disrupted by the E884K substitution from the acidic glutamic acid (E) to the basic lysine (K). The E884–R958 salt bridge is present in the kinase domain crystal structures complexed to either erlotinib or lapatinib. (**c**) Superposition of the EGFR kinase domain with the catalytic domains of diverse kinases shows structural conservation of a buried Glu(E)–Arg(R) ion pair. The crystal structure of EGFR tyrosine kinase (PDB accession code: 1M17) (Stamos *et al.*, 2002) was superimposed with the catalytic kinase domains of human CDK2 (PDB accession code: 1VYW) (Pevarello *et al.*, 2004), human JNK3 (PDB accession code: 1PMQ) (Scapin *et al.*, 2003), human insulin receptor kinase (PDB accession code: 1IR3) (Hubbard, 1997), ZAP-70 tyrosine kinase (PDB accession code: 1U59) (Jin *et al.*, 2004), LCK kinase (PDB accession code: 1QPD) (Zhu *et al.*, 1999) and MET (PDB accession code: 2RFS) (Bellon *et al.*, 2008) using Cα atoms in the program DeepView/Swiss-PdbViewer v3.7. The conserved Glu–Arg ion pair is shown in stick format, with oxygen atoms colored red and nitrogens, blue. The EGFR side chains are shown in yellow. The structural location of the ion pair is conserved in these crystal structures and helps orientate helix αEF. Figures 4b and c were prepared using the program PYMOL (www.pymol.org).

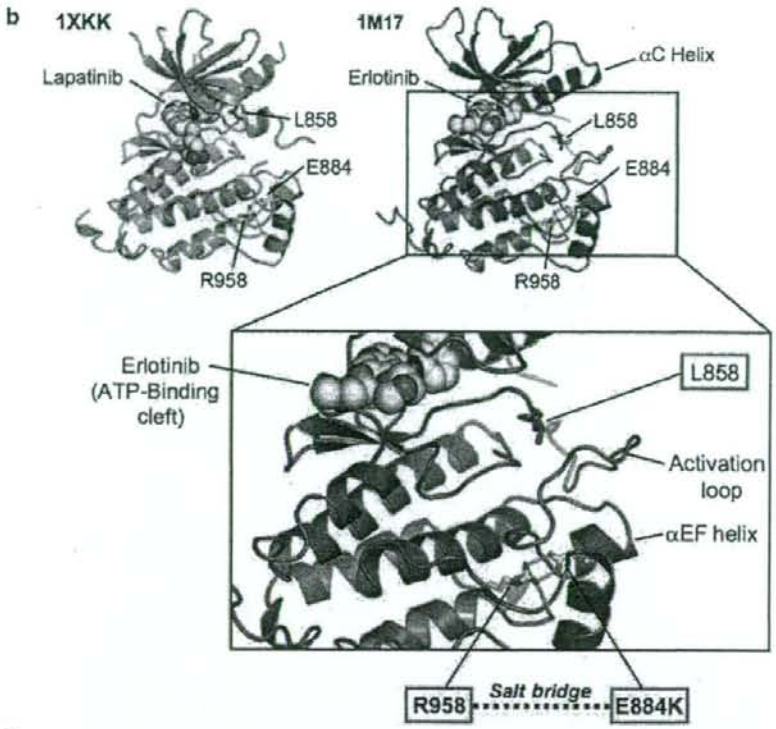

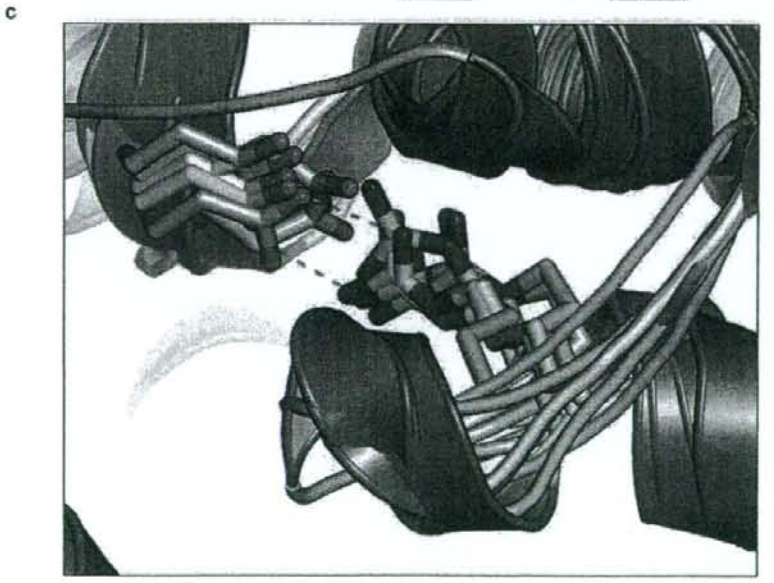

Figure 4 Continued.

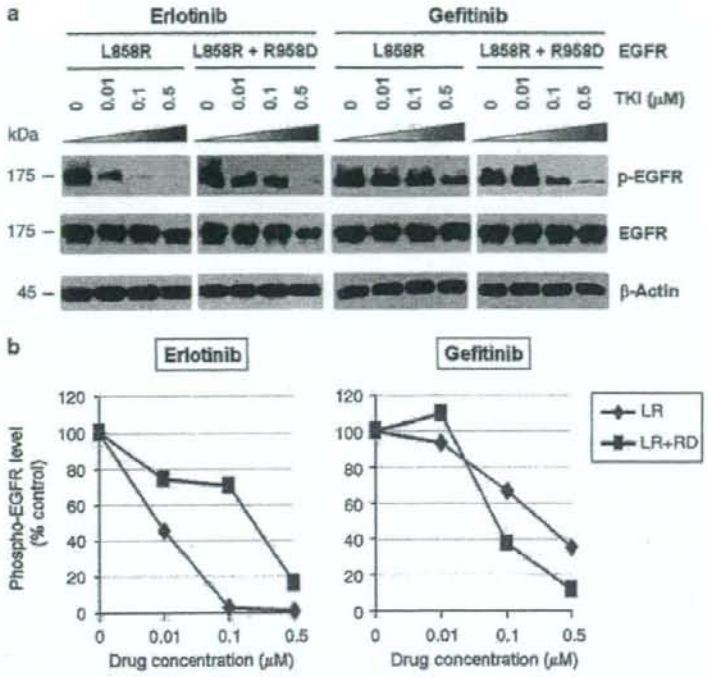

Figure 5 Disruption of the conserved Glu(E)884 Arg(R)958 salt bridge by a R958D substitution differentially altered L858R mutant receptor sensitivity to epidermal growth factor receptor (EGFR) inhibitors. (**a**) Stable COS-7 transfects expressing the sensitizing L858R and double-mutant L858R + R958D variants of EGFR were cultured in 0.5% bovine serum albumin-containing serum-free media for 16 h, and then incubated with increasing concentrations of either erlotinib or gefitinib, in the presence of EGF stimulation (100 ng/ml). Whole-cell lysates were extracted for SDS polyacrylamide gel electrophoresis and immunoblotted using antibodies against the followings: p-EGFR (Y1068), EGFR and β-actin. R958D mutation modulated the effect of L858R on inhibitor sensitivity resulting in desensitization of the mutant receptor to erlotinib inhibition but modestly enhanced sensitivity to gefitinib inhibition. (**b**) Densitometric quantitation of the p-EGFR (Y1068) levels showing that R958D mutation differentially altered L858R mutant receptor sensitivity to erlotinib (more resistant) and gefitinib (more sensitive). Densitometric scanning of the immunoblot signals shown in (**a**) was performed using NIH ImageJ software program, with normalization to total EGFR expression levels.

2008). Stable COS-7 transfectant cells expressing similar levels of wild type and E1271K-*MET* were used in this experiment using the two reversible preclinical MET inhibitors SU11274 (Ma *et al*., 2005a) and PHA665752 (Ma *et al*., 2005a, b). We did not find any significant modulation of sensitivity to SU11274 inhibition in the E1271K-MET cells (Figure 6b). On the other hand, the E1271K mutation of MET enhanced the sensitivity of inhibition by PHA665752 in the phosphorylation of the mutant MET at its major autophosphorylation sites (pY1234/1235) (equivalent to pY1252/1253 phosphosites as in the full-length *MET* transcript, with a difference of 18 amino acids in the exon 10 with the common alternatively spliced variant) in the kinase domain, and its downstream signaling proteins AKT and ERK1/2 (Figure 6b). Hence, disrupting the MET kinase salt bridge by the E1271K mutation also differentially alters sensitivity to MET kinase inhibitors in an inhibitor-specific manner.

Mutations at the conserved Glu(E)–Arg(R) ion pair in the human kinome

As the E884K somatic mutation was originally identified in a never-smoker woman of Japanese descent, we performed mutational screening for the presence of mutation at the E884 and R958 residues of *EGFR* among a cohort of 67 lung tumor genomic DNA specimens from Japanese non-small-cell lung cancer patients (including 66 transbronchial biopsies and 1 surgical specimen). Nonsynonymous mutations were not present in either residue location in this patient cohort. On the basis of our results suggesting the conserved structure and function of the Glu(E)–Arg(R) ion pair in EGFR and among other kinases in the kinome, we hypothesized that there would be other cancer-associated mutations at the conserved ion pair within the human kinome in kinases other than EGFR. Here, we performed bioinformatics survey of the updated Catalog of Somatic Mutations In Cancer (COSMIC) database (http://www.sanger.ac.uk/genetics/CGP/cosmic/) containing

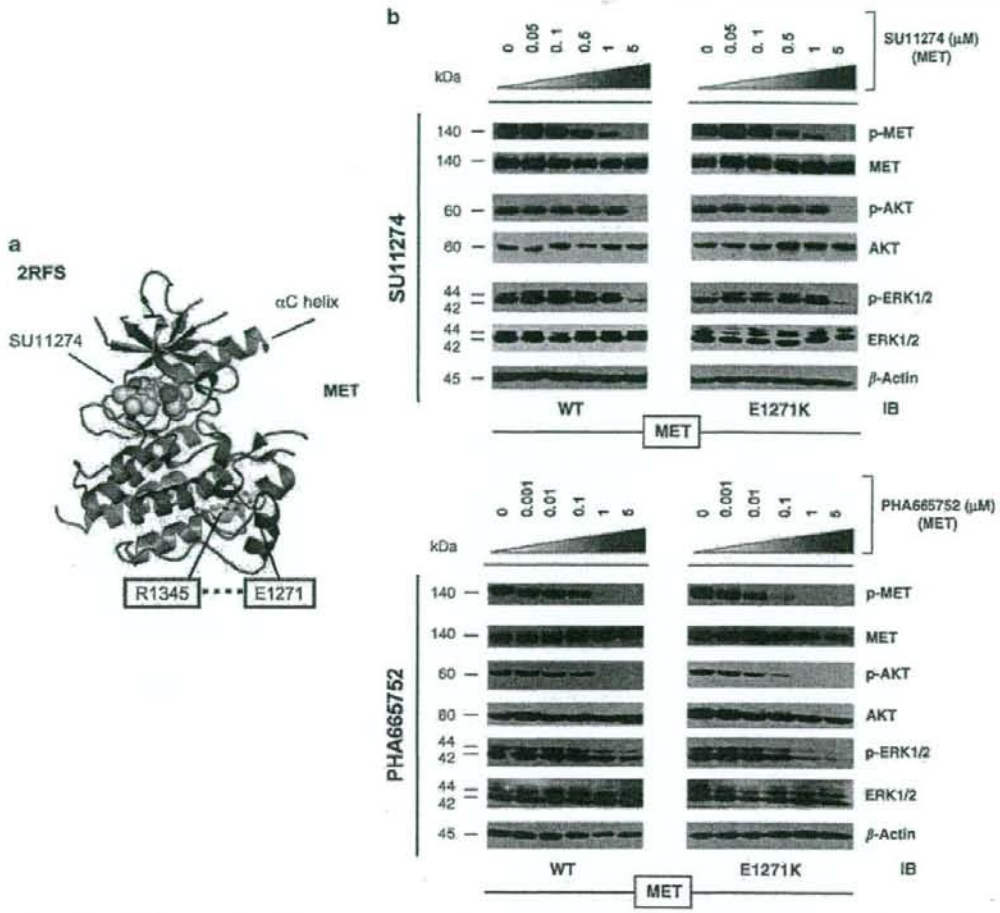

Figure 6 Mutational disruption of the conserved E1271 R1345 ion pair in MET kinase salt bridge causes inhibitor-specific modulation of sensitivity to SU11274 (unchanged) and PHA665752 (more sensitive). (a) MET kinase domain crystal structure (PDB accession code: 2RFS) (Bellon *et al*., 2008) highlighting the salt bridge between E1271 and R1345. Crystal structure solved in complex with SU11274 is shown. The conserved Glu Arg ion pair is shown in stick format, with oxygen atoms colored red, nitrogen atoms colored blue and carbon atoms colored yellow. This figure was prepared using the program PYMOL (www.pymol.org). (b) Stable COS-7 transfects expressing E1271K mutant *MET* were cultured in 0.5% bovine serum albumin-containing serum-free media for 16 h, then incubated with increasing concentrations of the MET inhibitors SU11274 (top) and PHA665752 (bottom) as indicated, in the presence of HGF stimulation (50 ng/ml). Whole-cell lysates were extracted for immunoblotting using antibodies against p-MET (Y1234/Y1235), MET, p-AKT, AKT, p-ERK1/2, ERK1/2 and β-actin. Wild-type *MET*-expressing COS-7 transfectant cells were included as control. E1271K mutation of MET increased the sensitivity of MET kinase phosphorylation inhibition by PHA665752.

somatic mutations identified in kinases among human cancers (Figure 7). We have conducted a complete and comprehensive survey throughout the entire human kinome for mutations identified at the conserved Glu(E)–Arg(R) ion pair in COSMIC. We also documented here the hits identifying mutations clustered in the vicinity of the ion pair, 30 amino acids proximal or distal to the Glu(E) or Arg(R). Interestingly, several kinases within the kinome were found to have mutations occurred at the Glu(E) residue, homologous to the E884–EGFR residue. These include KIT (E839K), RET (E921K), STK11/LKB1 (E223*). These are all known cancer-associated kinases that have dysregulated signaling in various human cancers, including GIST and hematological malignancies (KIT), papillary thyroid cancer (multiple endocrine neoplasm syndrome type 2) (RET) and lung cancer (RET, LKB1).

Discussion

In the era of molecularly targeted therapeutics in cancer therapy, the impact of cancer-associated mutations on kinase inhibitor sensitivity-resistance has increasingly

A[a]

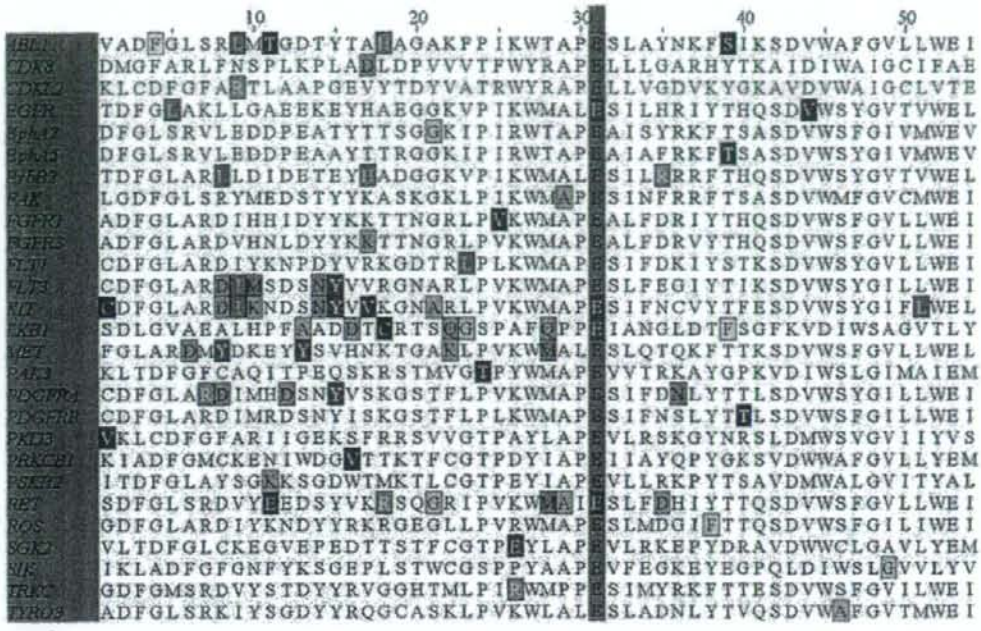

b

GENES	Mutations
ABL1:	F382L, L387M, T389A, H396P, H396R, S417Y
CDK8:	D189N
CDKL2:	R149Q
EGFR:	L858R, ***E884K***, V897I
EPHA2:	G777S
EPHA5:	T856I
ERBB2:	L869Q, H878Y, R896C
FAK:	***A612V***
FGFR1:	V664L
FGFR3:	K650E, K650M, K650Q, K650T
FLT1:	L1061V
FLT3:	D835E, D835F, D835H, D835N, D835V, D835Y, I836F, I836M, I836S, M837P, N841H, N841K, Y842C
KIT:	C809G, C809R, A814S, A814T, D816A, D816E, D816F, D816G, D816H, D816I, D816N, D816V, D816Y, I817V, K818R, D820E, D820G, D820H, D820N, D820V, D820Y, N822H, N822K, N822T, N822Y, Y823C, Y823D, Y823N, V825A, V825I, A829P, ***E839K***, L859P
LKB1:	A205T, D208N, C210*, Q214*, G215D, ***Q220****, ***E223****, F231L
MET:	D1246H, Y1248C, Y1248H, Y1253D, K1262R, ***M1268I***, ***M1268T***
PAK3:	T425S
PDGFRA:	R841S, D842*, D842I, D842V, D842Y, D846Y, Y849C, N870S
PDGFRB:	T882I
PKD3:	V716M
PRKCB1:	V496M
PSKH2:	K212I
RET:	E901K, R908K, G911D, ***M918T***, ***A919V***, ***E921K***, D925H
ROS:	F2138S
SGK2:	E259K
SIK:	G211S
TRKC:	R721F
TYRO3:	A709T

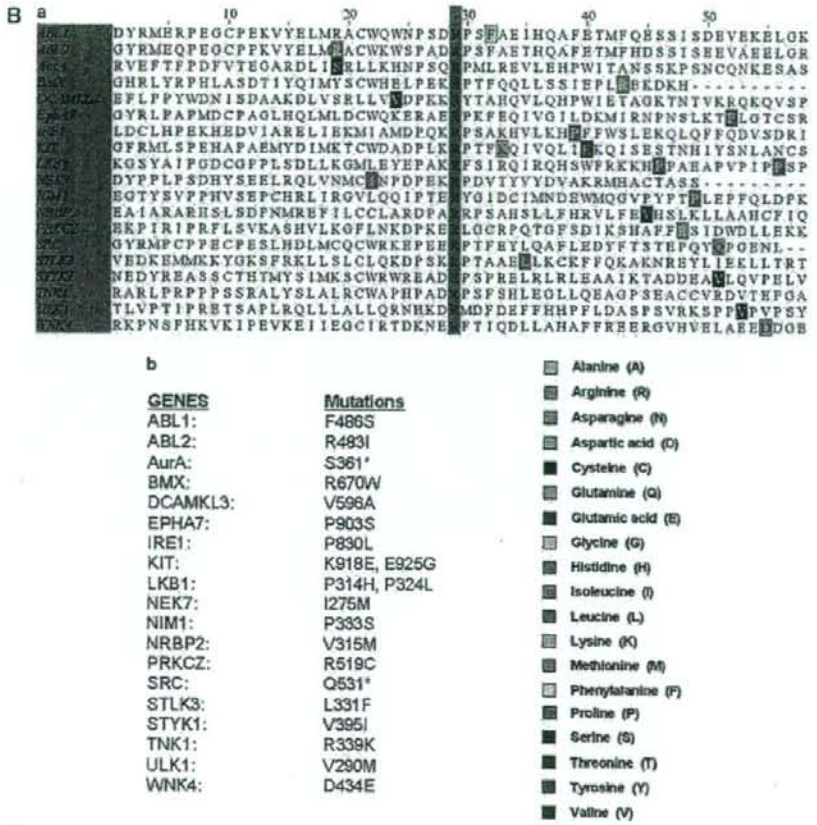

Figure 7 Continued.

important implications in the success of novel targeted inhibitors such as erlotinib (EGFR-TKI). Furthermore, knowledge of mutational correlation with inhibitor sensitivity-resistance would most likely facilitate more effective and 'personalized' targeted therapeutics development in cancer therapy. The clinical course of the patient where the somatic E884K mutation was identified (Choong *et al*., 2006) suggested that different mutations of a target kinase, such as EGFR, may lead to differential responses to targeted kinase inhibitors. Alternatively, one may postulate that there might be differences in cerebrospinal fluid penetrance by TKIs that could potentially account for central nervous system failure with disease progression in the compartment on therapy (Jackman *et al*., 2006). Our biochemical studies here now show that E884K mutation in-*cis* with L858R differentially altered inhibitor sensitivity when compared with L858R alone, through differential inhibition of the pro-survival AKT and STAT3 signaling pathways associated with altered induction of cleaved-PARP(Asp214). This is also shown to occur in an inhibitor-specific manner within the class of various

Figure 7 Survey of identified mutations at the conserved salt bridge ion pair in the human kinome (COSMIC). The COSMIC database for the human cancer genome resequencing was surveyed and screened for potential mutations identified at or near the conserved Glu(E) Arg(R) salt bridge ion pair in the human kinome. (**A**) (a) Glu(E)884-EGFR and analogous alignment in the kinome. (b) List of the mutations identified in the kinome is included as reference. (**B**) (a) Arg(R)958-EGFR and analogous alignment in the kinome. (b) List of the mutations identified in the kinome is included as reference. The color code for the amino acids is included here. We have identified several kinases within the kinome that have mutations occurred at the Glu (E) residue, homologous to the E884-EGFR. These include KIT (E839K), RET (E921K) and LKB1 (E223*). These are all known oncogenic kinases that have dysregulated signaling in various human cancers, including GIST and hematological malignancies (KIT), papillary thyroid cancer (multiple endocrine neoplasm syndrome type 2) (RET) and lung adenocarcinoma (RET, LKB1). Whereas *KIT* and *RET* are oncogenes, *LKB1* has been shown to be a tumor-suppressor gene in lung cancer, and here we showed clustering of truncation mutations at and near the salt bridge ion pair as a result of a number of mostly nonsense mutations among some missense mutations. Although no mutation at E1271-*MET* was found, there are frequent clustered hotspots of mutations at its close vicinity: three amino-acid residues proximally at M1268 (M1268T/I). This is a known activating mutation of *MET* frequently associated with metastatic lesions promoting tumor motility and progression. The selected kinases with positive 'mutational hits' in our kinome bioinformatics screen are shown here for illustration.

ERBB family small-molecule inhibitors, including reversible single EGFR or dual inhibitors (gefitinib, erlotinib, lapatinib, 4557W, GW583340 and Tyrphostin-AG1478) and irreversible EGFR inhibitor (CL-387,785).

Moreover, the E884K alone and L858R + E884K double-mutant EGFR remained sensitive to EGF, and the E884K mutation cooperates with L858R when in-*cis* to enhance the mutational effects on downstream phosphoprotein activation. To date, essentially all mutational combinations involving L858R studied were found to exist in-*cis*, suggesting potential *cis* mutation-to-mutation cooperation in EGFR signaling and possibly tumorigenesis (Tam *et al.*, 2006). Interestingly, the double mutation L858R + E884K conferred a distinctly more sensitive response to EGF stimulation selectively in the MAPK-ERK1/2 cell proliferation pathway compared with either wild type, E884K alone or L858R alone. Hence, the double mutation L858R + E884K modulated downstream EGFR signaling differentially with distinctly different effects on the AKT (downregulated) and MAPK-ERK1/2 phosphorylation (upregulated). Moreover, E884K had a dominant effect over L858R, when in-*cis*, in these signaling modulatory effects. E884K, alone or in-*cis* with L858R, can also mediate induction of p-STAT3 (pY705) (important for STAT3 dimerization and transcriptional activation of target genes) and may have a role in differential regulation of STAT3 activation and thus nuclear translocation for transcriptional activity (Lo *et al.*, 2005). Our data also share some similarities to the recent findings that various activating 'gain-of-function' mutations of FLT3 showed differential downstream signaling activation along the STAT3, STAT5, AKT and MAPK-ERK1/2 pathways, whereas all induced FLT3 kinase activation constitutively (Frohling *et al.*, 2007). *EGFR* somatic doublet mutations are potentially more frequent than understood previously, with majority of them representing driver/driver mutations rather than driver/passenger mutations (Chen *et al.*, 2008). Future kinome-targeted therapies should take into account oncogenic effects of doublet mutations in the targets, and detailed analysis of the identified doublet mutations would be warranted.

Through sequence bioinformatics and structural analysis, we identified that the E884–R958 ion pair in EGFR kinase domain is highly conserved, by both sequence homology and structural salt-bridge formation, across the entire human kinome. Many of the protein kinases in the human kinome are 'druggable' therapeutic targets for various human cancers (Krause and Van Etten, 2005; Ma *et al.*, 2005a). This striking finding provides a structural basis for the potential mechanism of alteration of substrate specificity. This hypothesis is substantiated by our study using mutational disruption of the E884–R958 ion pair through an R958D substitution resulting in an opposite electrostatic charge between the wild-type and the mutant residue at codon 958. Similar differential sensitivity toward gefitinib (more sensitive) and erlotinib (more resistant) was observed in our *in vitro* EGFR inhibition study here. It is interesting to note that this salt bridge is located directly between two regions critical for normal EGFR activation, the intermolecular EGFR activation interface and the activation loop. Residue R958 falls between helices αH and αI and is proximal to the intermolecular EGFR activation interface recently revealed by structure-directed studies (Zhang *et al.*, 2006). Residue E884 is the conserved glutamate of the MALE motif (MAPE in PKA) and falls within helix αEF at the C terminus of the activation loop. This salt bridge helps to orientate helix αEF. In the recent EGFR kinase domain crystal structure bound to a peptide substrate analog (PDB accession code: 2GS6) (Zhang *et al.*, 2006), helix αEF packs against the substrate analog, suggesting that disruption of the salt bridge by an acquired E884K mutation could influence substrate recognition and binding. The acquisition of a lysine at codon 884 may therefore bring about local conformation disruptions that alter EGFR interactions with downstream substrates. Although we did not identify further E884K mutation (or any mutations involving R958 residue) in *EGFR* from the Japanese patients tumor sample cohort, the results of our study may have implication on the potential impact of cancer-associated mutations that may interrupt the integrity of the salt bridge of a kinase. As the human kinome is a rich source of 'druggable' targets, we extended our search through bioinformatics data-mining from the COSMIC human cancer genome resequencing project. To this end, we identified several proximal ion pair residue substitutions recorded in the COSMIC database at the E884 (EGFR) homologous residue, in the oncogenic kinases KIT and RET as well as in the tumor-suppressor LKB1 (also known as STK11). Mutations at the neighboring residues of the conserved motif MAPE(884), as exemplified in FAK-A612V, MET-M1268I/T, RET-M918T and RET-A919V, as well as the truncational nonsense mutation in LKB1-Q220*, were also identified from the COSMIC database. Furthermore, the juxtaposing proximal region to the MAPE(884) conserved motif in the kinome also appears to harbor mutational hotspots in the human cancer genome. Nonetheless, the significance of these mutations with respect to the kinase structure and signaling function is not clear. Although KIT has been extensively characterized with an established oncogenic role in some hematological malignancies and GIST, it has not been found to play a key role in lung cancer. However, recent studies have implicated interesting oncogenic role of RET (Thomas *et al.*, 2007), FAK (Ma *et al.*, 2007; Rikova *et al.*, 2007), MET (Ma *et al.*, 2005a) and tumor-suppressor role of LKB1 (Ji *et al.*, 2007) in lung cancer.

Recently, better understanding of signaling network interactions between EGFR and MET is beginning to emerge (Guo *et al.*, 2008; Tang *et al.*, 2008). MET genomic oncogenic amplification has also been identified to correlate with acquired resistance to EGFR inhibitors (gefitinib/erlotinib) with or without T790M-*EGFR* mutation (Bean *et al.*, 2007; Engelman *et al.*, 2007). Numerous kinase domain mutations of *MET* have been identified in previous studies, many of them shown to be activating and most frequently found in

metastatic tumor lesions compared with the primaries (Di Renzo *et al.*, 2000). The E1271–MET conserved ion pair residue occurs within the conserved MALE motif, where M1268 is a mutational hotspot frequently found substituted in human cancers (M1268T/I). This is a known activating mutation of *MET* frequently associated with metastatic lesions promoting tumor motility and progression. Our results here demonstrate that E1271K-MET effectuated differential effect on sensitivity toward the two preclinical MET inhibitors, SU11274 (unchanged) and PHA665752 (sensitizing). Hence, mutations in the kinase domain of MET may play a role in modulating the inhibitory spectrum of MET inhibitors, similar to what is established in EGFR-targeted therapy using gefitinib/erlotinib. Whether these mutationally specific differences in inhibitor sensitivity would eventually be clinically relevant is not clear at present and should be a focus of future research. MET is emerging as an important therapeutic target in cancer therapy beyond EGFR. More detailed studies to better define the relative role of kinase mutations in *MET* and how they can modulate inhibitor sensitivity would be warranted. Furthermore, nonkinase mutations of *MET*, in the extracellular sema domain and the short cytoplasmic juxtamembrane domain, have been identified to be important in lung cancer and mesothelioma (Ma *et al.*, 2003a, 2005a; Jagadeeswaran *et al.*, 2006). Little is known about the correlation of inhibitor sensitivity with these nonkinase mutations, and they should be included in future studies. Bellon *et al.* (2008) recently compared the crystal structures of a novel MET inhibitor AM7, and that of SU11274 when bound to the unphosphorylated form of MET kinase. They identified a novel binding mode of a MET inhibitor AM7 compared with SU11274 and raised the possibility of designing TKIs that have improved specific activity and specificity toward different mutant profiles in different cancers; hence 'mutationally-targeted inhibitors'.

Although the role of kinase domain mutations in modulating the sensitivity-resistance to small-molecule inhibitors, in the case of BCR/ABL, KIT and EGFR, has been quite extensively studied, in-depth understanding of the relative role of mutations in other target kinases, such as MET, RET and FAK in determining specific inhibitor sensitivity is still largely lacking. The ion pair formed by residues E884 and R958 in the EGFR kinase domain is a highly conserved feature in the human kinome, and mutations of this conserved ion pair may result in conformational changes that alter kinase substrate recognition. The discovery that disruption of the conserved E884–R958 ion pair affects EGFR signal transduction and inhibitor sensitivity indicates the clinical importance of *in vitro* and biochemical analysis for all documented resistance mutations. Our analysis also suggests that targeted therapy using small-molecule inhibitors should take into account potential cooperative effects of multiple intramolecular kinase mutations. As the number of targeted TKIs available increases, it is anticipated that a 'personalized' approach to cancer therapy on the basis of knowledge of the activating mutations present should improve the efficacy of these treatments.

Materials and methods

Plasmid constructs and site-directed mutagenesis

The plasmids pcDNA3.1 containing the full-length wild-type *EGFR* and the L858R-*EGFR* cDNA insert was a generous gift from Dr Stanley Lipkowitz (NIH/NCI). The generation of the kinase domain missense mutations of *EGFR*, E884K, L858R + E884K and L858R + R958D were performed using the QuikChange Site-Directed Mutagenesis XL II kit (Stratagene, La Jolla, CA, USA) as described previously (Choong *et al.*, 2006). The E1271K mutation of *MET* was introduced into the wild-type *MET* plasmid (Ma *et al.*, 2003a). Incorporation of the correct mutations was confirmed by direct DNA sequencing of the constructs.

Cell culture and transfection

COS-7 cells were grown as described previously (Choong *et al.*, 2006). Transfection method was described in Supplementary Materials and methods.

Cell proliferation and cytotoxicity assays

Cell proliferation and cytotoxicity assays were performed using tetrazolium compound-based CellTiter 96 AQ_{ueous} One Solution Cell Proliferation (MTS) assay (Promega) (see Supplementary Materials and methods).

Preparation of cell lysates and immunoblotting

Whole-cell lysates were extracted, separated by 7.5% SDS–polyacrylamide gel electrophoresis , immunoblotted using the various primary antibodies indicated and developed with SuperSignal West Pico Chemiluminescent Substrate (Pierce, Rockford, IL, USA) as described previously (Choong *et al.*, 2006). The following primary antibodies were used: phosphotyrosine (4G10, Upstate Biotechnology, Lake Placid, NY, USA), phospho-EGFR (Y1068) (BioSource International, Camarillo, CA, USA), EGFR (Santa Cruz Biotechnology, Santa Cruz, CA, USA), phospho-STAT3 (Y705) (Cell Signaling, Danvers, MA, USA), STAT3 (Zymed, South San Francisco, CA, USA), phospho-AKT (S473) (Cell Signaling), AKT (Biosource International), phospho-ERK1/2 (T202/Y204) (Cell Signaling), ERK1/2 (Biosource International), cleaved-PARP(Asp214) (cleaved-poly (ADP-ribose) polymerase (Asp214)) (Cell Signaling) and β-actin (Santa Cruz Biotechnology).

Chemicals

The details regarding the EGFR TKIs and MET TKIs used in this study are described in the Supplementary Materials and methods.

Lung tumor genomic DNA extraction and DNA sequencing

Genomics DNA was extracted using standard techniques from 67 non-small-cell lung cancer patients treated from July 1995 to March 2003 at Osaka Prefectural Medical Center for Respiratory and Allergic Disease (Osaka, Japan). All tumor samples were used in accordance with Institutional Review Board protocol, with patients' informed consent wherever necessary. Screening for mutations within exon 22 (harboring E884) and exon 23 (harboring R958) was performed using standard single-strand conformational polymorphism analysis, followed by direct DNA sequencing when indicated (for details, see Supplementary Materials and methods).

Bioinformatics sequence analysis

Multiple sequence alignments of kinase domains in the human kinome were performed for 321 human kinase domains. The positions of the conserved glutamate (E) and arginine (R) residues are colored purple and those of EGFR are indicated in red. FASTA files for human kinase domains were obtained from the kinase database at Sugen/Salk (Kinbase, La Jolla, CA, USA) and aligned with the AliBee multiple sequence alignment program (GeneBee) (Brodsky *et al*., 1992) using Clustal format. Resulting alignments were colored using JalView 2.2 (Clamp *et al*., 2004) according to sequence conservation (BLOSUM62). In addition, the amino-acid sequences from a selected list of 32 diverse human protein kinases were obtained from the ENSEMBL database (www.ensembl.org). The amino-acid sequences of these kinase domains were analysed and aligned using the EMBL-EBI online CLUSTALW software (www.ebi.ac.uk/clustalw).

Structural analysis

EGFR crystal structures (PDB accession codes 1M17, 1XKK and 2GS6) (Stamos *et al*., 2002; Wood *et al*., 2004; Zhang *et al*., 2006) were analysed using the program O (Jones *et al*., 1991). Superposition of the EGFR kinase domain with the catalytic domains of diverse kinases was performed to study the structural conservation of a buried Glu(E)–Arg(R) ion pair. The crystal structure of EGFR tyrosine kinase (PDB accession code: 1M17) (Stamos *et al*., 2002) was superimposed with the catalytic kinase domains of human CDK2 (PDB accession code: 1VYW) (Pevarello *et al*., 2004), human JNK3 (PDB accession code: 1PMQ) (Scapin *et al*., 2003), human insulin receptor kinase (PDB accession code: 1IR3) (Hubbard, 1997), ZAP-70 tyrosine kinase (PDB accession code: 1U59) (Jin *et al*., 2004), LCK kinase (PDB accession code: 1QPD) (Zhu *et al*., 1999) and MET (PDB accession code: 2RFS) (Bellon *et al*., 2008) using Cα atoms in the program DeepView/Swiss-PdbViewer v3.7. Figures were prepared using the program PYMOL (www.pymol.org).

Abbreviations

COSMIC, catalogue of somatic mutations in cancer; EGFR, epidermal growth factor receptor; MAPK (ERK1/2), mitogen-activated protein kinase (extracellular signaling-regulated kinase 1/2); STAT3, signal transducer and activator of transcription 3; TKI, tyrosine kinase inhibitor.

Acknowledgements

Patrick C Ma is supported by NIH/National Cancer Institute-K08 Career Development Award (5K08CA102545-04), American Cancer Society (Ohio)-Institutional Research Grant (IRG-91-022, Case Comprehensive Cancer Center) and Ohio Cancer Research Associates (Give New Ideas A Chance) Grant Award. Titus J Boggon is an American Society of Hematology Junior Faculty Scholar. Edward T Petri is supported by an NIH/National Cancer Institute T32 training Grant (5T32CA009085-32). We thank Dr Zhenghe J Wang (Department of Genetics, Case Western Reserve University) for critically reading the manuscript and for helpful suggestions.

References

Bean J, Brennan C, Shih JY, Riely G, Viale A, Wang L *et al*. (2007). MET amplification occurs with or without T790M mutations in EGFR mutant lung tumors with acquired resistance to gefitinib or erlotinib. *Proc Natl Acad Sci USA* **104**: 20932 20937.

Bellon SF, Kaplan-Lefko P, Yang Y, Zhang Y, Moriguchi J, Rex K *et al*. (2008). c-Met inhibitors with novel binding mode show activity against several hereditary papillary renal cell carcinoma related mutations. *J Biol Chem* **283**: 2675 2683.

Brodsky LI, Vasiliev AV, Kalaidzidis YL, Osipov YS, Tatuzov RL, Feranchuk SI. (1992). GeneBee: the program package for biopolymer structure analysis. *Dimacs* **8**: 127 139.

Chen Z, Feng J, Saldivar JS, Gu D, Bockholt A, Sommer SS (2008). EGFR somatic doublets in lung cancer are frequent and generally arise from a pair of driver mutations uncommonly seen as singlet mutations: one-third of doublets occur at five pairs of amino acids. *Oncogene* **27**: 4336 4343.

Choong NW, Dietrich S, Seiwert TY, Tretiakova MS, Nallasura V, Davies GC *et al*. (2006). Gefitinib response of erlotinib-refractory lung cancer involving meninges—role of EGFR mutation. *Nat Clin Pract Oncol* **3**: 50 57; quiz 51 p following 57.

Clamp M, Cuff J, Searle SM, Barton GJ. (2004). The Jalview Java alignment editor. *Bioinformatics* **20**: 426 427.

Di Renzo MF, Olivero M, Martone T, Maffe A, Maggiora P, Stefani AD *et al*. (2000). Somatic mutations of the MET oncogene are selected during metastatic spread of human HNSC carcinomas. *Oncogene* **19**: 1547 1555.

Engelman JA, Zejnullahu K, Mitsudomi T, Song Y, Hyland C, Park JO *et al*. (2007). MET amplification leads to gefitinib resistance in lung cancer by activating ERBB3 signaling. *Science* **316**: 1039 1043.

Frohling S, Scholl C, Levine RL, Loriaux M, Boggon TJ, Bernard OA *et al*. (2007). Identification of driver and passenger mutations of FLT3 by high-throughput DNA sequence analysis and functional assessment of candidate alleles. *Cancer Cell* **12**: 501 513.

Guo A, Villen J, Kornhauser J, Lee KA, Stokes MP, Rikova K *et al*. (2008). Signaling networks assembled by oncogenic EGFR and c-Met. *Proc Natl Acad Sci USA* **105**: 692 697.

Hubbard SR. (1997). Crystal structure of the activated insulin receptor tyrosine kinase in complex with peptide substrate and ATP analog. *Embo J* **16**: 5572 5581.

Jackman DM, Holmes AJ, Lindeman N, Wen PY, Kesari S, Borras AM *et al*. (2006). Response and resistance in a non-small-cell lung cancer patient with an epidermal growth factor receptor mutation and leptomeningeal metastases treated with high-dose gefitinib. *J Clin Oncol* **24**: 4517 4520.

Jagadeeswaran R, Ma PC, Seiwert TY, Jagadeeswaran S, Zumba O, Nallasura V *et al*. (2006). Functional analysis of c-Met/hepatocyte growth factor pathway in malignant pleural mesothelioma. *Cancer Res* **66**: 352 361.

Ji H, Ramsey MR, Hayes DN, Fan C, McNamara K, Kozlowski P *et al*. (2007). LKB1 modulates lung cancer differentiation and metastasis. *Nature* **448**: 807 810.

Jin L, Pluskey S, Petrella EC, Cantin SM, Gorga JC, Rynkiewicz MJ *et al*. (2004). The three-dimensional structure of the ZAP-70 kinase domain in complex with staurosporine: implications for the design of selective inhibitors. *J Biol Chem* **279**: 42818 42825.

Jones TA, Zou JY, Cowan SW, Kjeldgaard M. (1991). Improved methods for building protein models in electron density maps and the location of errors in these models. *Acta Crystallogr A* **47**(Part 2): 110 119.

Kobayashi S, Boggon TJ, Dayaram T, Janne PA, Kocher O, Meyerson M *et al*. (2005). EGFR mutation and resistance of non-small-cell lung cancer to gefitinib. *N Engl J Med* **352**: 786 792.

Krause DS, Van Etten RA. (2005). Tyrosine kinases as targets for cancer therapy. *N Engl J Med* **353**: 172 187.

Lo HW, Hsu SC, Ali-Seyed M, Gunduz M, Xia W, Wei Y *et al*. (2005). Nuclear interaction of EGFR and STAT3 in the activation of the iNOS/NO pathway. *Cancer Cell* **7**: 575 589.